GNSS Jammers: Effects and Countermeasures

Daniele Borio, Cillian O'Driscoll, Joaquim Fortuny,
EC Joint Research Centre, Institute for the Protection and Security of the Citizen, Ispra, Italy

***Abstract*—GNSS jammers are small portable devices able to broadcast disruptive interference and overpower the much weaker GNSS signals.**
In this paper, the effects of GNSS jammers on GPS and Galileo receivers are thoroughly analyzed and the use of an adaptive notch filter is suggested as an effective countermeasure to jamming. Signals generated by a commercial jammer are broadcast in a large anechoic chamber along with the GPS and Galileo signals generated by a hardware simulator. The analysis is conducted in terms of C/N_0 degradation and different jammer power levels are considered.
The use of mitigation techniques, such as notch filtering, significantly improves the performance of GNSS receivers even in the presence of strong and fast-varying jamming signals. The presence of a pilot tone in the Galileo E1 signal enables pure PLL tracking and makes the processing of Galileo signals more robust to jamming.

***Index Terms*—GNSS, GPS, Interference, Jammers, Notch Filter**

I. Introduction

Global Navigation Satellite System (GNSS) jammers are small portable devices able to broadcast disruptive signals in the GNSS bands. A jammer can overpower the much weaker GNSS signals and disrupt GNSS-based services in a geographical area with a radius of several kilometres [1]. Despite the fact that the use of such devices is illegal in most countries, jammers can be easily purchased on the Internet and their rapid diffusion is becoming a serious threat to satellite navigation.

A first study which analyzed the characteristics of the signals emitted by 18 Global Positioning System (GPS) jammers was presented in [1]. From the analysis, it emerged that signals broadcast by these devices are usually characterized by linear frequency modulations: the instantaneous frequency of the signal sweeps a range of several MHz in a few microseconds affecting the entire GNSS band targeted by the device. Recently, [2] studied the impact of two jammers on several commercial GPS receivers. The results presented in [2] are in line with the findings provided by [1] and confirm that GNSS jammers can corrupt GNSS signal reception over wide geographical areas.

The analyses provided by [1], [2] were limited to GPS signals in the L1 and L2 frequencies. Moreover, the main focus was the characterization of the interfering signals and their impact on commercial receivers. The problem of mitigating the effect of interfering signals was only marginally considered in [2].

The main focus of this paper is thus the analysis of possible countermeasures to GNSS jammers. GNSS interference detection and mitigation have been the focus of intense research activities and several techniques have been developed to reduce the impact of specific disturbing signals [3]–[7]. For example, pulsed and Continuous Wave Interference (CWI) received particular attention from the scientific community. CWI can be easily generated by faulty electronics whereas pulsed signals can be produced by services operating in the GNSS bands [8]. The mitigation of chirp interference, i.e. that caused by a linear frequency modulation, has received relatively little attention due to the reduced probability of unintentionally generating these signals.

In this paper, adaptive notch filtering [6], [7] is considered for mitigating the effects of GNSS jammers. It is noted that despite adaptive notch filtering having been widely used for the mitigation of CWI, the analysis of its performance in the presence of a chirp signal is still missing in the literature. The ability of the adaptive notch filter to track the frequency variations of a chirp signal has not been previously analyzed. The analysis has been conducted using a commercial jammer and a Spirent GSS8800 hardware simulator able to generate GPS and Galileo L1 signals. The signal generated by the commercial jammer has been broadcast in a large anechoic chamber along with GNSS signals generated by hardware simulator. The Spirent hardware simulator was also used to evaluate the impact of GNSS jammers on Galileo receivers. The GNSS and interfering signals were recorded using a National Instruments (NI) Radio-Frequency (RF) signal analyzer (NI PXI-5663) and processed using commercial and software-based GNSS receivers. A variable attenuator was used to test the effect of different interference power levels and better analyze the behavior of the notch filter. The analysis was conducted in terms of Carrier-to-Noise density power ratio (C/N_0) degradation following a procedure similar to that adopted in [9] to assess the impact of LightSquared interference on commercial GPS receivers.

From the analysis it emerges that the use of mitigation techniques, such as the notch filter, significantly improves the performance of GNSS receivers even in the presence of strong jamming signals. More specifically, it is shown that although the structure of chirp signals can pose problems to the adaptive notch filter, a significant performance increase can be obtained if the notch adaptation algorithm is fast enough to track the chirp. The adaptive notch filter is generally able to track continuous frequency variations even if frequency jumps, which occur when the jammer reaches its maximum signal frequency, can introduce transients and biases in the frequency estimated by the notch filter. However, the residual interference power is usually located far from the GPS/Galileo L1 centre frequency and it is removed during the standard correlation process. Finally, the performance of

the notch filter can be further improved by properly tuning the algorithm parameters.

The remainder of this paper is organized as follows. In Section II, the signal model adopted is briefly reviewed whereas the adaptive notch filter used for this study is briefly reviewed in Section III. Section Section IV discuss the approach adopted for testing the impact of a commercial GPS jammer and analyzing the effects of the notch filter. Experimental results are provided in Section V and conclusions are presented in Section VI.

II. Signal Model

The signal at the input of a GNSS receiver in a one-path additive Gaussian channel and in the presence of interference can be modeled as

$$r(t) = \sum_{l=0}^{L-1} y_l(t) + i(t) + \eta(t), \tag{1}$$

which is the sum of L useful signals transmitted by L different satellites, the interfering signal, $i(t)$, generated by the GPS jammer and a noise term, $\eta(t)$. Each useful signal, $y_l(t)$, can be expressed as

$$\begin{aligned} y_l(t) = \sqrt{2C_l} d_l\left(t-\tau_{0,l}\right) c_l\left(t-\tau_{0,l}\right) \\ \cdot \cos\left(2\pi(f_{RF}+f_{0,l})t+\varphi_{0,l}\right), \end{aligned} \tag{2}$$

where

- C_l is the power of the lth useful signal;
- $d_l(\cdot)$ is the navigation message;
- $c_l(\cdot)$ is the lth pseudo-random sequence extracted from a family of quasi-orthogonal codes and used for spreading the signal spectrum;
- $\tau_{0,l}$, $f_{0,l}$ and $\varphi_{0,l}$ are the delay, Doppler frequency and phase introduced by the communication channel;
- f_{RF} is the centre frequency of the GNSS signal.

In (1), $i(t)$ can assume different forms depending on the type of jammer. Several recent studies [1], [2], [10], have investigated the temporal and statistical characteristics of $i(t)$ and a brief summary is provided in Section II-A.
Due to the quasi-orthogonality of the spreading codes, a GNSS receiver is able to process the L useful signals independently and (2) can be simplified to

$$r(t) = y(t) + i(t) + \eta(t), \tag{3}$$

where the index, l, has been dropped for ease of notation.
The signal (3) is filtered and down-converted by the receiver front-end before being digitized. Digitization implies two different operations: sampling and amplitude quantization. In the following, it is assummed that the fron-end Analog-to-Digital Converter (ADC) performs signal digitization using a significant number of bits (at least 8) and the effects of quantization are neglected. In addition, it is assumed that the signal is sampled without introducing significant distortions. After down-conversion and sampling, (3) becomes:

$$r_{BB}[n] = y_{BB}(nT_s) + i_{BB}(nT_s) + \eta_{BB}(nT_s) \tag{4}$$

where the notation $x[n]$ is used to denote a discrete time sequence sampled at the frequency $f_s = \frac{1}{T_s}$. The index "BB" is used to denote a signal down-converted to base-band. In (4), $y_{BB}[n]$ is defined as

$$y_{BB}[n] = \sqrt{C} d\left(nT_s-\tau_0\right) c\left(nT_s-\tau_0\right) \exp\left\{j2\pi f_0 nT_s + j\varphi_0\right\}. \tag{5}$$

The noise term, $\eta_{BB}[n]$, is assumed to be complex Additive White Gaussian Noise (AWGN) with independent and identically distributed (i.i.d.) real and imaginary parts with variance σ^2. This variance depends on the filtering, down-conversion and sampling strategy applied by the receiver front-end and is given by $\sigma^2 = N_0 B_{Rx}$, where B_{Rx} is the front-end one-sided bandwidth and N_0 is the Power Spectral Density (PSD) of the input noise, $\eta(t)$. The ratio between the carrier power, C, and the noise power spectral density, N_0, defines the C/N_0, one of the main signal quality indicators used in GNSS. It is noted that the C/N_0 is a property of the received signal and does not depend on the receiver adopted for the processing. The C/N_0 is however usually unknown and needs to be estimated. In particular, a GNSS receiver determines the signal C/N_0 by estimating at first the Signal-to-Noise Ratio (SNR) at the correlator outputs. A model, relating the SNR to the C/N_0, is then used to calculate the C/N_0 from the SNR. This model does not usually account for the presence of interference, implementation losses and other degradations that a GNSS receiver can experience. For this reason, the C/N_0 estimated by the receiver is indeed an effective C/N_0 accounting for different degradations such as the effect of interference [11], [12]. In the following, the effect of a jammer will be quantified as the degradation in effective C/N_0 due to the presence of an interfering signal. This type of methodology is commonly used in the literature [9] and allows one to quantify the equivalent noise increase caused by an interfering signal.

A. GPS Jammer Signal Model

The down-converted interference signal, $i_{BB}(nT_s)$, can assume different forms depending on the jammer which generates it and the effect of the GNSS receiver front-end. Several efforts have been devoted to the analysis and characterization of civilian GPS jammers [1], [2], [10] and, despite significant differences, the transmitted signal is usually frequency modulated with an almost constant amplitude. The time-frequency evolution of the signal transmitted by a car GPS jammer is shown in Fig. 1 along with its instantaneous received power. In this case, the instantaneous frequency of interfering signal evolves linearly over the interval $[f_{L1}+f_{\min}, f_{L1}+f_{\max}]$ where f_{L1} is the GPS L1 centre frequency and $f_{min} \approx -7$ MHz, $f_{max} \approx 5.5$ MHz. It is noted that the instantaneous frequency of $i_{BB}(nT_s)$ follows a periodic pattern and a reset occurs every $T_i \approx 9$ μs. Signal power variations occur in correspondence of a reset.
From the previous discussion, it emerges that $i_{BB}(nT_s)$ can be approximately modeled as

$$i_{BB}(nT_s) = A_i \exp\left\{j2\pi\Phi(nT_s)nTs + j\varphi_i\right\} \tag{6}$$

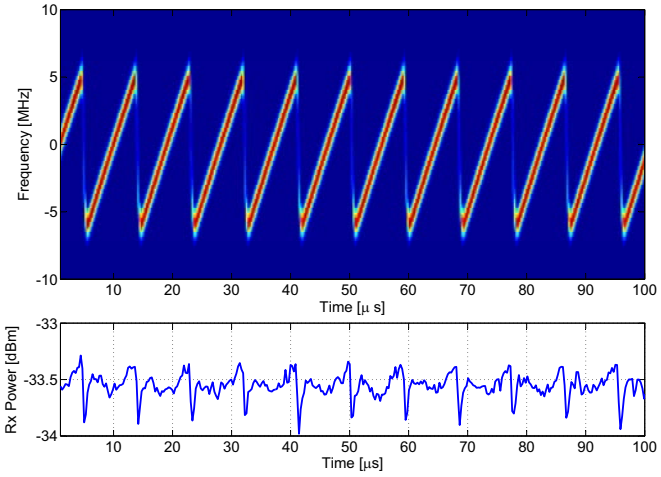

Fig. 1. Time-frequency evolution of the signal transmitted by a car GPS jammer. The instantaneous received signal power is provided in the bottom part of the figure.

where A_i is the interfering signal amplitude, $\Phi(nT_s)$ is its time-varying frequency and φ_i the initial phase. It is noted that (6) neglects several signal properties and more complex models can be adopted [10]. Model (6) is however able to capture the most important feature of $i_{BB}(nT_s)$, i.e., the fact that it is instantaneously narrow band. The fact that $i_{BB}(nT_s)$ is instantaneously narrow band is exploited in Section III to design interference mitigation techniques that can reduce the impact of the signal transmitted by the jammer.

III. Adaptive Notch Filter

Several interference mitigation techniques are available in the literature [3]–[6] and are generally based on the interference cancellation principle. These techniques attempt to estimate the interference signal, which is subsequently removed from the input samples. For example, transform domain excision techniques [4] at first project the input signal onto a domain where the inference signal assumes a sparse representation. The interference signal is then estimated from the most powerful coefficients of the transformed domain representation. The interfering signal is removed and the original signal representation is restored. When the signal is narrow band, Discrete Fourier Transform (DFT)-based frequency excision algorithms [4] are particularly effective. Despite their effectiveness, transform domain excision techniques are computationally demanding and other mitigation techniques have been considered in the literature. For example, notch filters are particularly effective for removing CWI.

In this paper, the adaptive notch filter considered in [6], [7] is used to reduce the impact of the signal generated by a commercial GPS jammer. This technique has been selected for its reduced computational requirements and for its good performance in the presence of CWI and due to the fact that commercial jammers produce a swept CWI. The notch filter considered in this paper has been extensively tested in the presence of CWI, however its performance in the presence of frequency modulated signals has not been assessed.

The notch filter considered in this work is characterized by the following transfer function [7]:

$$H_n(z) = \frac{1 - z_0[n]z^{-1}}{1 - k_\alpha z_0[n]z^{-1}} \tag{7}$$

where k_α is the pole contraction factor and $z_0[n]$ is the filter zero. k_α controls the width of the notch introduced by the filter whereas $z_0[n]$ determines the notch centre frequency. It is noted that $z_0[n]$ is progressively adapted using a Least Mean Squares (LMS) approach [13] with the goal of minimizing the energy at the output of the filter. A thorough description of the adaptation algorithm is out of the scope of the paper and details can be found in [6], [7].

The notch filter [6] is able to place a deep null in correspondence of the instantaneous frequency of a narrow band interference and, if the zero adaptation parameters are properly chosen, to track the interference frequency variations. It is possible to show that if the LMS algorithm used for updating $z_0[n]$ is able to reach steady state then

$$\hat{\Phi}(nT_s) = \frac{f_s}{2\pi}\angle z_0[n] \approx \Phi(nT_s) \tag{8}$$

which implies that $z_0[n]$ can be used to estimate the instantaneous frequency of interfering signal, $i_BB(nT_s)$. In [7], it is also shown that the magnitude of $z_0[n]$ strongly depends on the amplitude of the interfering signal, A_i. Indeed, $|z_0[n]|$ monotonically converges to 1 as A_i increases. Thus, $|z_0[n]|$ can be used to detect the interference presence and the notch filter can be used only if $|z_0[n]|$ passes a predefined threshold, T_z. This approach is used in this paper where a threshold $T_z = 0.75$ has been empirically selected.

The performance of the notch filter in the presence of a GPS jammer is discussed in the next sections.

IV. Experimental Setup

To test the capability of the adaptive notch filter to mitigate against a typical in-car jammer, an experiment was conducted in a large anechoic chamber at the Joint Research Centre (JRC). The experimental setup is shown schematically in Fig. 2. The anechoic chamber provides a completely controlled environment in which all sources of interference besides the jammer under test can be eliminated. In addition, by performing the tests in the chamber, it can be ensured that the jammer does not have an adverse affect on any GNSS receivers in the vicinity of the test site.

A Spirent GSS8800 simulator was used to provide a controlled GPS and Galileo constellation, with a static receiver under nominal open sky conditions. The GNSS signals were broadcast from an Right Hand Circular Polarization (RHCP) antenna mounted on a movable sled on the ceiling of the chamber. A survey grade GNSS antenna was mounted inside the chamber and the sled was positioned at a distance of approximately 10 metres from this antenna. The GNSS receiving antenna was connected via a splitter to a spectrum analyzer, an RF down-converter digitizer and a commercial

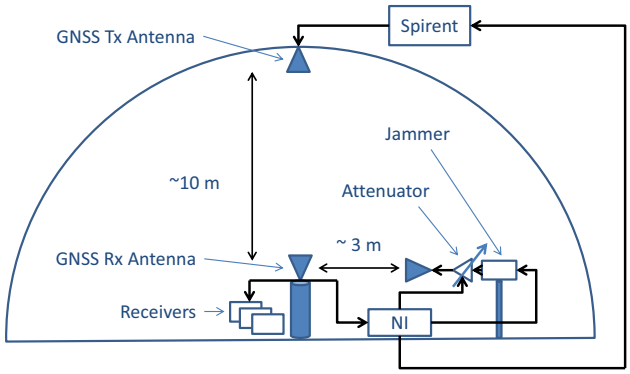

Fig. 2. Schematic of the experimental setup

TABLE I
DOWN CONVERTER/DIGITIZER PARAMETERS

Parameter	Value
Centre Frequency	1575.42 MHz
Sampling Rate	10 MHz
Sample Type	Complex
Bits Per Sample	16
Bandwidth	$\approx$ 10 MHz

high sensitivity GPS receiver. The down-converter digitizer parameters are recorded in Table I.

To provide the source of jamming signals a commercially available (though illegal) in-car jammer was connected to a programmable power supply. The jammer's antenna was removed and the antenna port was connected, via a programmable attenuator with up to 81 dB of attenuation, to a calibrated standard gain horn antenna. This gain horn was positioned at approximately 2 metres from the GNSS receiving antenna. The goal of this configuration was to permit variation of the total jammer power received at the antenna. Unfortunately, the jammer itself is very poorly shielded, such that a significant amount of the interfering power that is seen by the receiver was found to come directly from the body of the jammer, rather than through the antenna. Thus great care was exercised to shield the jammer as much as possible from the GNSS antenna. The jammer body was placed in an aluminium box, which was subsequently surrounded by RF absorbent material. The jammer body and the receiving GNSS antenna were separated by approximately 15 m thereby ensuring approximately 60 dB of free space path loss.

The experiment was controlled via a National Instruments PXI controller, which generated synchronous triggers for the RF data collection and Spirent signal generation, controlled the power supplied to the jammer and updated the attenuation settings according to a desired profile. All events (trigger generation, jammer power on/off, attenuation setting) were time stamped using an on-board timing module. The commercial receiver was configured to log raw GPS measurements including C/N_0.

The experimental procedure involved two trials, each lasting

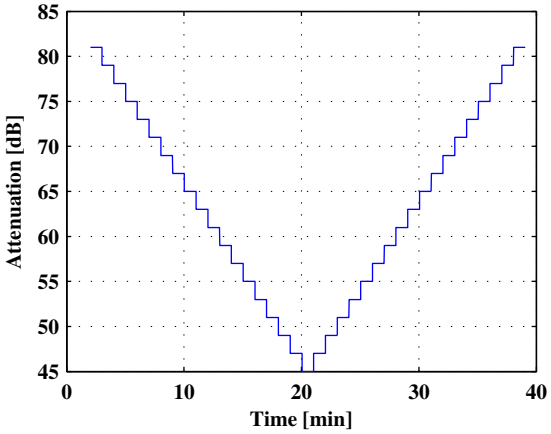

Fig. 3. Attenuation profile applied to the jammer signal during the experiment

approximately 40 minutes. In the first the simulator and data collection equipment were both enabled, but the jammer remained powered off. In the second trial, the same scenario was generated in the simulator, the data collection equipment was enabled and, after a period of 3 minutes, the jammer was powered on. The attenuation was initially set to its maximum value of 81 dB. This was subsequently reduced in 2 dB decrements to a minimum value of 45 dB. Each level was maintained for a period of 60 s. Finally, the attenuation was again increased in 2 dB increments to its maximum value. This attenuation profile is shown in Fig. 3.

In reality, the attenuation level is not a useful parameter in understanding the behaviour of either the jammer or the chosen mitigation strategy. To this end a calibration procedure was performed whereby the total received jammer power at the output of the active GNSS receiving antenna was measured using a calibrated spectrum analyzer while the attenuation level was varied. In addition, the total noise power was measured in the same 12 MHz bandwidth with the jammer switched off. This permitted the computation of the received Jammer-to-Noise density power ratio (J/N_0) as a function of the attenuator setting. The result of this procedure is illustrated in Fig. 4. The analysis in the next section is conducted using J/N_0 as a measure of the impact of the jammer.

V. RESULTS

Fig. 5 shows the loss in C/N_0 experienced in the presence of the jammer as a function of J/N_0. The first is obtained from the software receiver processing of the GPS signals, the second from software receiver processing of the Galileo signals and the third is obtained from a commercial receiver which processed only the GPS signals. The first point to note is that there is little difference between the GPS and Galileo results. This is to be expected due to the wideband nature of the jammer. In fact, for both GPS and Galileo processing the jammer is effectively averaged over many chirp periods, thereby giving it the appearance of a broadband (white) noise source. The one difference between the GPS and Galileo signals is that the tracking threshold of the Galileo signals is

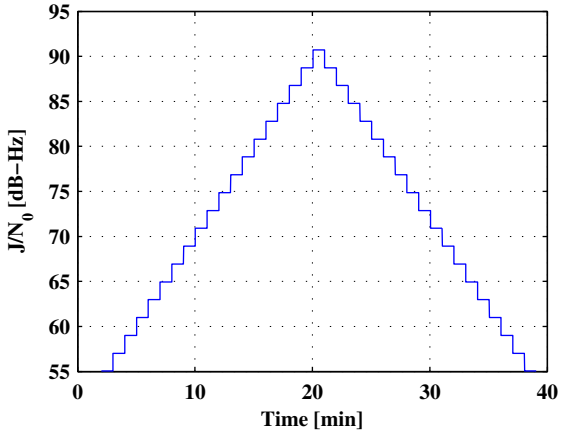

Fig. 4. Calibrated J/N_0 at the output of the active GNSS antenna vs time.

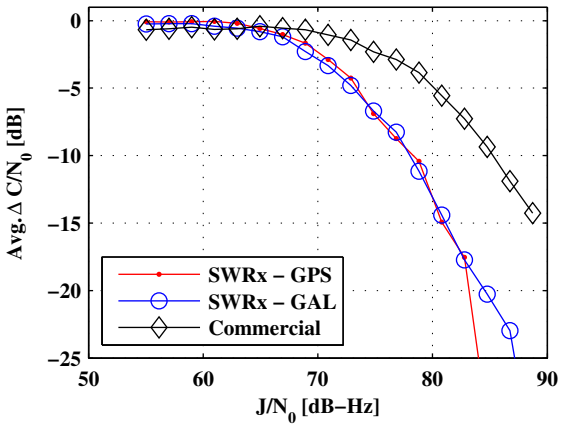

Fig. 5. Average C/N_0 loss vs J/N_0 for: a) software receiver processing of GPS; b) software receiver processing of Galileo; c) a commercial High Sensitivity GPS receiver.

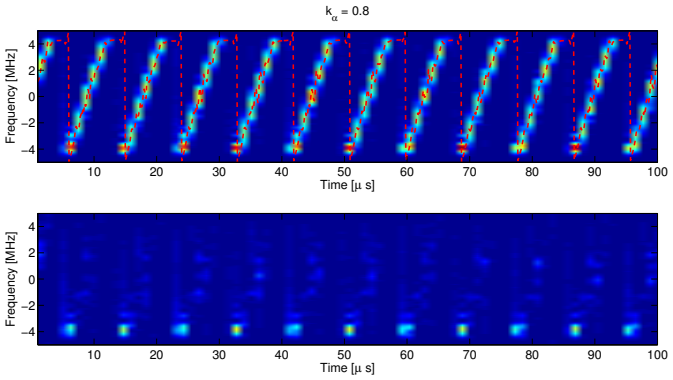

Fig. 6. Time-frequency evolution of the received and notched ($k_\alpha = 0.8$) signals. The top plot shows the raw data with the estimated interference frequency obtained from the notch filter superimposed in red. The bottom plot shows the filtered data.

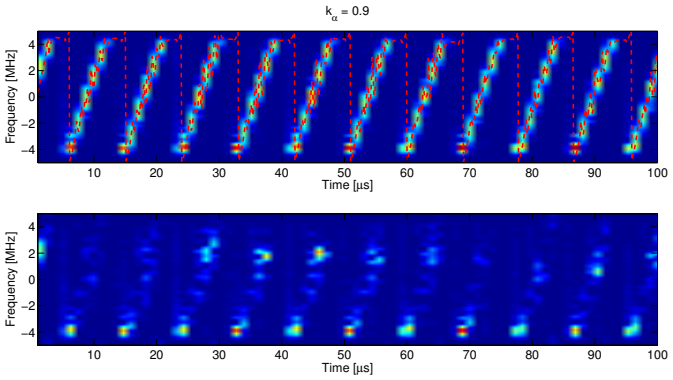

Fig. 7. Time-frequency evolution of the received and notched ($k_\alpha = 0.9$) signals. The top plot shows the raw data with the estimated interference frequency obtained from the notch filter superimposed in red. The bottom plot shows the filtered data.

approximately 6 dB lower than that for the GPS signals. This is due to the use of a pure Phase Lock Loop (PLL) processing strategy using only the E1C (pilot) component of the Galileo signal.

The other interesting point to note from Fig. 5 is that the commercial receiver exhibits better resilience against the jammer. This is most likely due to a narrower front-end bandwidth in the commercial reciever, though this cannot be confirmed since the receiver manufacturer does not provide this information. As seen in Fig. 1 above, the bandwidth of the jammer signal is approximately 10 MHz. The bandwidth of the digitized RF data is also approximately 10 MHz. If the commercial receiver has a smaller bandwidth, then it would effectively filter out some of the jammer power, thereby improving its performance with respect to the software receiver results.

Two configurations of the adaptive notch filter were tested: 1) $k_\alpha = 0.8$; 2) $k_\alpha = 0.9$. The first case has a smaller contraction factor and hence a wider notch than the latter. The adaptive step size of the LMS algorithm was tuned for the jammer under consideration (the filter must be sufficiently adaptive to account for the frequency variation of the jammer's chirp signal). In each case the location of the zero of the notch filter was used as a detector for interference. A threshold of 0.75 was chosen such that when the amplitude of the zero was greater than this threshold the notch filter was enabled and the receiver processed this filtered data. Otherwise the receiver processed the raw data collected from the antenna.

The result of the filtering is illustrated in Figs. 6 and 7 for the two cases. In these plots, the time evolution of the frequency content of the raw data is shown in the upper plot, with the frequency estimate of the notch filter superimposed as a dashed red line. The lower plots show the time evolution of the frequency content of the filtered data. From these lower plots it appears that the wider notch does a better job of removing the jammer signal. On the other hand, this will result in a greater reduction of the signal power also.

The ability of the adaptive notch filter to detect the jammer is illustrated in Fig. 8, which shows the evolution of the magnitude of the zero as a function of time. The amplitude is averaged of 4 ms and this averaged value is used as the

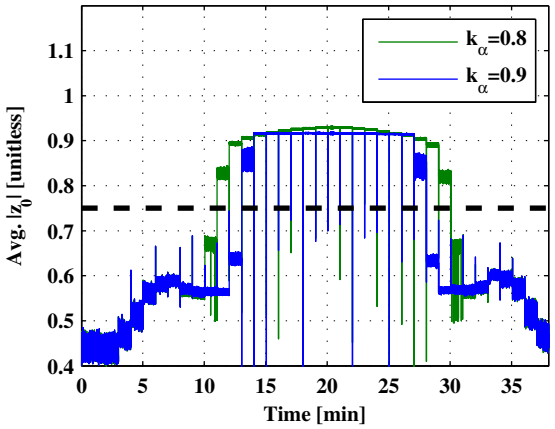

Fig. 8. Evolution of $\overline{|z_0|}$ vs time: a) $k_\alpha = 0.8$; b) $k_\alpha = 0.9$. The dashed black line denotes the threshold used to switch between processing the filtered and unfiltered data.

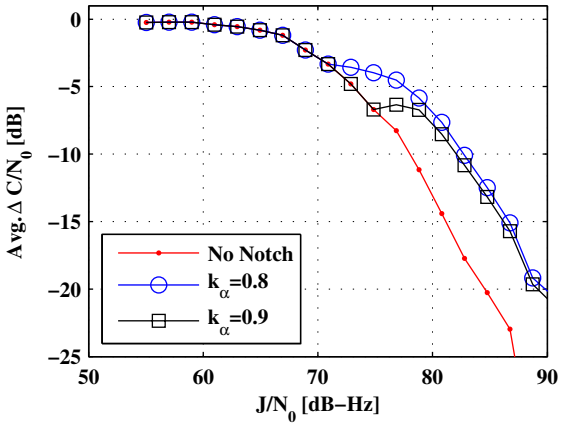

Fig. 9. Average Galileo C/N_0 loss vs J/N_0 for: a) no notch filtering; b) notch filtering with $k_\alpha = 0.8$; c) $k_\alpha = 0.9$

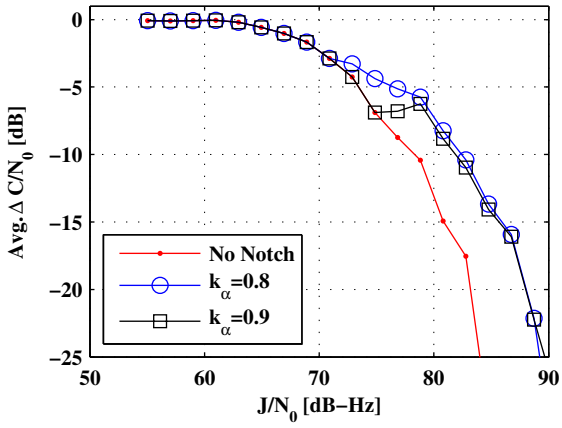

Fig. 10. Average GPS C/N_0 loss vs J/N_0 for: a) no notch filtering; b) notch filtering with $k_\alpha = 0.8$; c) $k_\alpha = 0.9$

threshold for enabling the notch filter. The step changes in received jammer power are clearly visible, indicating that this metric is a useful indicator of the presence of a jammer. The sudden "dips" in the absolute value of the zero correspond to resets of the adaptive algorithm. It was found that the adaptive algorithm tends to diverge when there are sudden abrupt changes in the received jammer power so a divergence test was included in the algorithm. It is interesting to note that the lower contraction factor implementation resulted in the jammer being switched "on" at an earlier stage (lower J/N_0) than the higher.

The impact of the notch filter on the GNSS signals is illustrated in Figs. 9 and 10, which show the impact of the notch filter on the C/N_0 degradation for Galileo and GPS signals respectively. Again, the difference between the impact on GPS and Galileo signals is slight, due to the wideband nature of the interferer. On the other hand, the benefit of the notch filter is clear in both figures. Interestingly, it appears that there are two limiting curves: one for the case of no filtering and one for the case where a notch filter is applied. The variation in the contraction factor (over the range considered) has little impact on the the effective C/N_0. The separation between the two curves is approximately 5 dB, *i.e.* the receiver that applies the notch filter experiences approximately 5 dB less C/N_0 loss than an unprotected receiver for the same J/N_0. Of course, it must be borne in mind that this result applies for the data collection system considered in this test, which consists of a 14 bit ADC with no Automatic Gain Control (AGC). In practical receivers the non-linear losses due to the combination of these two front-end components will likely lead to additional losses.

VI. Conclusion

The adaptive notch filter has been proposed as an easy to implement mitigation technique for jammers generating chirp signals, typical of the type of commercially available jammer that has become ever more present in recent years. A simple LMS adaptation algorithm was implemented, with an associated simple interference detection scheme. It was shown that, for a receiver with sufficient dynamic range, the proposed technique leads to an improvement of approximately 5 dB in terms of effective C/N_0. The proposed scheme was tested on data collected from a low cost commercial jammer in a large anechoic chamber. Processing was conducted using a software receiver operating on both GPS and Galileo signals. The broadband nature of the chirp signal means that its impact on GNSS signal processing is similar to an increase in the thermal noise floor. Hence, the impact is very similar on GPS and Galileo. On the other hand, the chirp signal is instantaneously narrowband: a feature that is exploited by the use of a notch filter with a highly dynamic response to variations in the frequency of the interferer.

The present work is a preliminary demonstration of the suitability of the adaptive notch filter in mitigating the effects of commercial GNSS jammers. Future work will focus on a more thorough assessment of the degradation induced by the notch filter itself, investigation of the choice of the threshold

T_z for interference detection and more advanced adaptation algorithms.

REFERENCES

[1] R. H. Mitch, R. C. Dougherty, M. L. Psiaki, S. P. Powell, B. W. O'Hanlon, J. A. Bhatti, and T. E. Humphreys, "Signal characteristics of civil GPS jammers," in *Proc. of the 24th International Technical Meeting of The Satellite Division of the Institute of Navigation (ION GNSS)*, Portland, OR, Sep. 2011, pp. 1907–1919.

[2] H. Kuusniemi, E. Airos, M. Zahidul, H. Bhuiyan, and T. Kroger, "Effect of GNSS jammers on consumer grade satellite navigation receivers," in *Proc. of the European Navigation Conference (ENC)*, Gdanks, Poland, Apr. 2012, pp. 1–14.

[3] V. Calmettes, F. Pradeilles, and M. Bousquet, "Study and comparison of interference mitigation techniques for GPS receiver," in *Proc. of the 14th International Technical Meeting of the Satellite Division of The Institute of Navigation (ION GPS 2001)*, Salt Lake City, UT, Sep. 2001, pp. 957–968.

[4] J. Young and J. Lehnert, "Analysis of DFT-based frequency excision algorithms for direct-sequence spread-spectrum communications," *IEEE Trans. Commun.*, vol. 46, no. 8, pp. 1076 –1087, Aug. 1998.

[5] R. Landry, V. Calmettes, and M. Bousquet, "Impact of interference on a generic GPS receiver and assessment of mitigation techniques," in *Proc. of the 5th IEEE International Symposium on Spread Spectrum Techniques and Applications*, vol. 1, Sep. 1998, pp. 87 –91.

[6] D. Borio, L. Camoriano, and L. Lo Presti, "Two-pole and multi-pole notch filters: A computationally effective solution for GNSS interference detection and mitigation," *IEEE Systems Journal*, vol. 2, no. 1, pp. 38 –47, Mar. 2008.

[7] D. Borio, "A statistical theory for GNSS signal acquisition," Doctoral Thesis, Dipartimento di Elettronica, Politecnico di Torino, http://plan.geomatics.ucalgary.ca/papers/phdthesis_danieleborio_02apr08.pdf, Apr. 2008.

[8] R. J. Landry and A. Renard, "Analysis of potential interference sources and assessment of present solutions for GPS/GNSS receivers," in *Proc. of the 4th St. Petersburg International Conference on Integrated Navigation Systems*, May 1997.

[9] Technical Working Group (TWG), "Lightsquared-GPS technical working group final report," Federal Communication Commission, Washington, D.C., Tech. Rep., Jun. 2011.

[10] R. H. Mitch, M. L. Psiaki, B. W. O'Hanlon, S. P. Powell, and J. A. Bhatti, "Civilian GPS jammer signal tracking and geolocation," in *Proc. of the 25th International Technical Meeting of The Satellite Division of the Institute of Navigation (ION GNSS)*, Nashville, TN, Sep. 2012.

[11] J. W. Betz, "Effect of partial-band interference on receiver estimation of C/N_0," in *Proc. of the 2001 National Technical Meeting of The Institute of Navigation*, Long Beach, CA, Jan. 2001, pp. 817 – 828.

[12] ——, "Effect of narrowband interference on GPS code tracking accuracy," in *Proc. of ION National Technical Meeting*, Anaheim, CA, Jan. 2000, pp. 16–27.

[13] S. Haykin, *Adaptive Filter Theory*, 4th ed. Prentice Hall, Sep. 2001.